Nonlinear, Low-Energy-Actuator-Prioritizing Control Allocation for Winged eVTOL UAVs

Mason B. Peterson
Electrical and Computer Engineering
Brigham Young University
Provo, USA
masonbp@byu.edu

Randal W. Beard
Electrical and Computer Engineering
Brigham Young University
Provo, USA
beard@byu.edu

Jacob B. Willis
Robotics Institute
Carnegie Mellon University
Pittsburgh, USA
jwillis2@andrew.cmu.edu

2022 Intermountain Engineering, Technology and Computing (IETC) | 978-1-6654-8653-8/22/$31.00 ©2022 IEEE | DOI: 10.1109/IETC54973.2022.9796842

***Abstract*—Winged eVTOL aircraft's ability to generate aerodynamic lift with wings and to create upward thrust with upward-facing rotors makes these vehicles capable of the kind of versatile flight needed in urban environments. Because of these vehicles' aerodynamic complexities and their unique methods of producing thrusts and torques, control allocation is needed to determine how to distribute force and torque efforts across the aircraft's actuators. However, current control allocation methods fail to properly represent the actuators' complex dynamics and are unable to harness the full potential of these over-actuated vehicles. Current shortcomings include modeling rotors as linear effectors while the wide range of airspeeds experienced by eVTOL aircraft leads to significant nonlinearities in the thrust and torque achieved by each rotor. This means linear control allocation methods may consistently fail to produce desired thrusts and torques, which can inhibit the vehicle from tracking a trajectory at best, and at worst can cause the vehicle to stall and lose control. Additionally, current control allocation methods are often unable to prioritize low-energy actuators resulting in shorter battery life. We present a nonlinear control allocation method that considers a nonlinear rotor model, allows for prioritization of low-energy control surfaces over rotors, and reliably accounts for actuator saturation. Simulation results show a 90% reduction in high-airspeed trajectory tracking position error from a typical, linear least-squares pseudoinverse control allocation method while maintaining comparable energy use.**

***Index Terms*—Electric vertical takeoff and landing (eVTOL), control allocation, aerospace control, unmanned aerial vehicle**

I. Introduction

Winged Electric Vertical Take-Off and Landing (eVTOL) aircraft are capable of tracking previously unachievable flight trajectories because of their unique ability to produce upward and forward thrust using rotors and lift using wings. This enables these vehicles to take-off vertically, transition to energy-efficient, fixed-wing flight, and then land, all without needing a runway or other ground-based infrastructure. These vehicles are subject to complex aerodynamics during transition to and from fixed-wing flight which has historically made autonomous control of these vehicles difficult. However, the large number of applications for Unmanned Air Vehicles (UAVs) with these capabilities has given rise to an increased focus on eVTOLs among the research community.

This work has been funded by the Center for Unmanned Aircraft Systems (C-UAS), a National Science Foundation Industry/University Cooperative Research Center (I/UCRC) under NSF award No. IIP-1650547, along with significant contributions from C-UAS industry members.

One specific area of research has been eVTOL control allocation. Control allocation, one of the final pieces of an autonomous controller, calculates actuator outputs needed to achieve a thrust and torque commanded by inner loops of the controller. Actuator effectiveness is often described using a control allocation matrix which maps actuators to corresponding thrust or torque produced along relevant body axes. A common solution for aircraft control allocation involves computing the minimum norm pseudoinverse of the control allocation matrix and then taking the matrix product of the pseudoinverse and the desired wrench vector to find the minimum-norm actuator setpoints that will achieve the desired thrust and torque, as described in [1] and discussed in Section III.

We previously addressed the eVTOL control allocation problem by creating an airspeed-dependent control allocation matrix and applying the pseudoinverse method to calculate actuator setpoints [2]. However, the linearization of rotor thrust and torque about hover throttles used in this this method does not accurately describe the thrust and torque produced at the high airspeeds needed for fixed-wing flight. Additionally, the pseudoinverse method does not account for actuator saturation. In [3], a weighted least squares algorithm is used to find actuator setpoints for eVTOLs while prioritizing achievement of thrust and roll- and pitch-inducing torque. While the method in [3] takes actuator saturation into account, it still uses a linear rotor model and is not capable of prioritizing certain actuators. In [4] the control allocation matrix is updated at each time-step using airspeed trimming, and an affine generalized inverse is used to compute more accurate actuator setpoints. The difference between the output setpoint vector and a desired, no-effort setpoint vector is also minimized to reduce energy use. This allows for actuator prioritization but still is ultimately using a linearized model. A control allocation algorithm is developed in [5] that precomputes a possible wrench space, and projects the desired thrust and torque onto this wrench space to find a thrust and torque that is attainable by the vehicle. This method is able to prioritize energy efficiency and thruster effort distribution, but does not account for nonlinearities in rotor models at high airspeeds.

In this paper, we present a control allocation scheme that handles actuator saturation, prioritizes efficient actuators, and

uses a nonlinear thrust model to represent rotor thrust with greater accuracy. This control allocation method builds off the controller presented in [2] which provides control for an eVTOL vehicle across its full flight using a single controller capable of handling the aircraft in hover, transition, and fixed-wing flights using all actuators throughout the duration of the flight. We show that our proposed control allocation method results in significant improvement over the control allocation method described in [2].

We begin with a discussion of our aerodynamic and propulsion models in Section II. In Section III we will present our novel, nonlinear control allocation technique for eVTOLs. Finally, in Section IV we will show our simulation results using AirSim, which we have adjusted to use our customized dynamics [6].

II. Aerodynamic Aircraft Model

The aerodynamic model we chose is a first-principles lumped element model. In particular, we note the nonlinear forces and moments that affect the aircraft and the unique challenges they pose for control of eVTOL vehicles. Not all of the aerodynamics experienced by a winged eVTOL are captured using this model, but it provides the fidelity we desire without being computationally burdensome. Aerodynamic effects not considered in this model include interaction between the rotors and wings, and unsteady flow due to vehicle geometry. Simulations of some of these effects were compared for a bi-wing tailsitter eVTOL in [7].

Throughout this paper the notation $\boldsymbol{r}^c_{a/b}$ is used to denote a vector quantity $\boldsymbol{r}$ of frame a with respect to frame b and expressed in frame c. Similarly, the notation $\varphi_{a/b}$ is used for an angle from frame b to frame a. We use i to refer to the north-east-down inertial frame, b to refer to the true body-fixed frame, and d to refer to the desired trajectory frame.

We denote the canonical unit vectors in $\mathbb{R}^3$ as $\boldsymbol{e}_1, \boldsymbol{e}_2$, and $\boldsymbol{e}_3$ and the $n \times n$ identity matrix as $I_{n\times n}$.

A. Tri-Tiltrotor Aircraft Model

We have chosen to demonstrate the use of our nonlinear, low-energy-actuator-prioritizing control allocation method with the E-flite Convergence tri-tiltrotor eVTOL vehicle. The Convergence UAV has seven actuators: two elevons, three rotors, and two servos that independently control the angle of the front rotors. The rear rotor is fixed and points in the $-\boldsymbol{z}_b$ direction of the aircraft body frame. A diagram showing the naming conventions for the vehicle actuators is shown in Figure 1.

The actuator inputs are rotor throttles $\boldsymbol{\delta}_r = [\delta_{r_1}, \delta_{r_2}, \delta_{r_3}]^\top$ where $\delta_{r_*} \in [0, 1]$, rotor angles $\boldsymbol{\xi}_r = [\xi_{r_1}, \xi_{r_2}, \xi_{r_3}]^\top$ where $\xi_{r_*} \in [0°, 115°]$ with $\xi_{r_3} = 90°$ and where ξ_{r_*} is a right-handed rotation from the positive x-axis about the y-axis, and where the elevon deflections $\boldsymbol{\delta}_e = [\delta_{e_1}, \delta_{e_2}]^\top$ where $\delta_{e_*} \in [-1, 1]$. The positions of the rotors in the vehicle body frame are written as $\boldsymbol{q}_i$, where $\boldsymbol{q}_i = [q_{i,x}, q_{i,y}, q_{i,z}]^\top$.

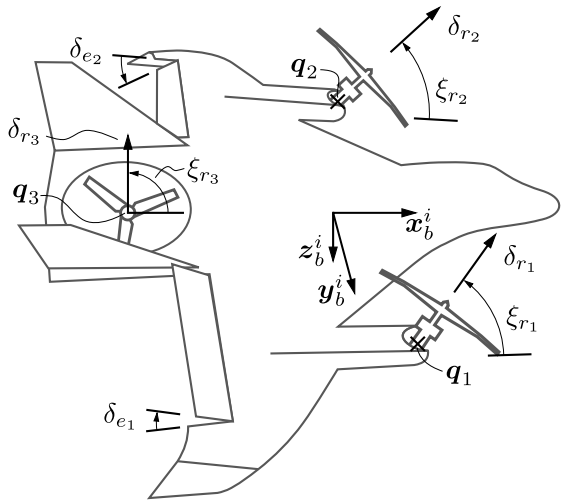

Fig. 1. Actuator notation for a tiltrotor eVTOL

B. eVTOL Aircraft Kinematics and Dynamics

The rigid body equations of motion of an eVTOL are given by

$$\dot{\mathbf{p}}^i_{b/i} = \mathbf{v}^i_{b/i} \tag{1a}$$

$$\dot{\mathbf{v}}^i_{b/i} = g\boldsymbol{e}_3 + \frac{1}{m} R^i_b \mathbf{F}^b_b \tag{1b}$$

$$\dot{R}^i_b = R^i_b \lfloor \boldsymbol{\omega}^b_{b/i} \rfloor_\times \tag{1c}$$

$$\dot{\omega}^b_{b/i} = -J^{-1} \lfloor \boldsymbol{\omega}^b_{b/i} \rfloor_\times J \boldsymbol{\omega}^b_{b/i} + J^{-1} \mathbf{M}^b_b, \tag{1d}$$

where $\mathbf{p} \in \mathbb{R}^3$ is the position of the aircraft's center of mass, $\mathbf{v} \in \mathbb{R}^3$ is the velocity of the aircraft, $\mathbf{F} \in \mathbb{R}^3$ is the non-gravitational external forces acting on the vehicle, $\mathbf{M} \in \mathbb{R}^3$ is the vector of moments experienced by the aircraft, $\boldsymbol{\omega} \in \mathbb{R}^3$ is the angular velocity of the vehicle, and $J \in \mathbb{R}^{3\times3}$ is the aircraft's inertia matrix. These equations of motion are the basis of the controller described in [2], which we use in conjunction with our control allocation method presented here. For control allocation, we are primarily concerned with the forces and moments acting on the vehicle. We describe the forces and moments acting in the aircraft body frame as

$$\begin{aligned}\mathbf{F}^b_b = \mathbf{F}_0(\mathbf{v}^b_{b/w}) + \mathbf{F}_\omega(\mathbf{v}^b_{b/w})\boldsymbol{\omega}^b_{b/i} \\ + \mathbf{F}_{\delta_e}(\mathbf{v}^b_{b/w})\boldsymbol{\delta}_e + \mathbf{F}_r(\mathbf{v}^b_{b/w}, \boldsymbol{\delta}_r, \boldsymbol{\xi}_r)\end{aligned} \tag{2}$$

$$\begin{aligned}\mathbf{M}^b_b = \mathbf{M}_0(\mathbf{v}^b_{b/w}) + \mathbf{M}_\omega(\mathbf{v}^b_{b/w})\boldsymbol{\omega}^b_{b/i} \\ + \mathbf{M}_{\delta_e}(\mathbf{v}^b_{b/w})\boldsymbol{\delta}_e + \mathbf{M}_r(\mathbf{v}^b_{b/w}, \boldsymbol{\delta}_r, \boldsymbol{\xi}_r),\end{aligned} \tag{3}$$

which are the composite of several nonlinear functions that depend on the aircraft's airspeed vector ($\mathbf{v}^b_{b/w}$), rotational velocity, and setpoints applied to the elevons ($\boldsymbol{\delta}_e$), rotors ($\boldsymbol{\delta}_r$), and tilt servos ($\boldsymbol{\xi}_r$). Here, $\mathbf{F}_0$ represents the force function of the aircraft due to the wing geometry, $\mathbf{F}_\omega$ is the force due to the rotation of the vehicle, $\mathbf{F}_{\delta_e}$ is the force from the aircraft's elevons, and $\mathbf{F}_r$ is the force due to the rotors. The moments follow a similar notation.

C. Actuator Model

While it is important for the full controller to model all the forces and moments acting on the vehicle, the control allocation deals only with the forces and torques the vehicle can produce using its rotors and control surfaces. Earlier pieces of the controller factor in the forces and moments due to aerodynamics and gravity when calculating desired forces and torques for the aircraft's actuators to produce.

We represent the force and torque produced by the vehicle's actuators with the equation

$$\mathbf{b}(\boldsymbol{\delta}, \mathbf{v}_{b/w}^b) = \begin{bmatrix} \mathbf{F}_{\delta_e}(\mathbf{v}_{b/w}^b)\boldsymbol{\delta}_e + \mathbf{F}_r(\mathbf{v}_{b/w}^b, \boldsymbol{\delta}_r, \boldsymbol{\xi}_r) \\ \mathbf{M}_{\delta_e}(\mathbf{v}_{b/w}^b)\boldsymbol{\delta}_e + \mathbf{M}_r(\mathbf{v}_{b/w}^b, \boldsymbol{\delta}_r, \boldsymbol{\xi}_r) \end{bmatrix}, \quad (4)$$

where $\mathbf{F}_{\delta_e} \in \mathbb{R}^2$ and $\mathbf{F}_r \in \mathbb{R}^2$ are composed of forces in the x_b- and z_b- axes. Forces in the y_b-axis are not included in this representation because the Convergence aircraft's actuators cannot produce force along this axis.

The linear control allocation method in [2] uses a linear approximation of $\mathbf{b}$ as

$$\mathbf{b}(\boldsymbol{\delta}, \mathbf{v}_{b/w}^b) \approx \mathbf{b}(\boldsymbol{\delta}_0, \mathbf{v}_{b/w}^b) + B\boldsymbol{\delta} \quad (5)$$

$$B = \left.\frac{\partial \mathbf{b}}{\partial \boldsymbol{\delta}}\right|_{\boldsymbol{\delta}=\boldsymbol{\delta}_0}, \quad (6)$$

where B is the Jacobian of $\mathbf{b}$ with respect to the actuator setpoint vector. Linear control allocation methods use the B matrix of constant coefficients multiplied by the actuator setpoint vector $\boldsymbol{\delta}$ to model the thrust/torque produced as shown in [1]. While this method is effective for vehicles that operate within low airspeeds, such as quadrotor aircraft, measures must be taken to achieve sufficient control of aircraft that operate at higher airspeeds and thus experience greater effects due to the nonlinearities of the rotors and control surfaces. So, we represent the full $\mathbf{b}$ function in our control allocation solution rather than just the Jacobian matrix B.

To account for thrust and torque differences at high airspeeds, we incorporate a nonlinear rotor model into our control allocation scheme. We represent the functions of thrust and torque achieved by a rotor as $T_p(\delta_r, \mathbf{v}_{b/w}^r)$ and $\Omega_p(\delta_r, \mathbf{v}_{b/w}^r)$ respectively, where $\mathbf{v}_{b/w}^r$ is the airspeed vector of the aircraft expressed in the rotor frame. $\mathbf{v}_{b/w}^r$ is found using the airspeed vector of the aircraft along with the servo setpoint of the tiltrotor and the position of the rotor. These functions use electrical constants describing the motor and aerodynamic constants of the propeller which are found experimentally. The function definitions are not included here due to space constraints, but can be found in [8].

The $\mathbf{b}(\boldsymbol{\delta}, \mathbf{v}_{b/w}^b)$ function is constructed using the geometry of the vehicle in combination with the nonlinear propulsion functions to calculate thrusts and torques achieved by each rotor. Our nonlinear control allocation scheme uses the following equations to compute the forces and torques achieved by a tri-tiltrotor eVTOL with actuator setpoints defined by the $\boldsymbol{\delta}$ vector, where $\boldsymbol{\delta} = [\delta_{r1}, \delta_{r2}, \delta_{r3}, \xi_{r1}, \xi_{r2}, \delta_{e1}, \delta_{e2}]^\top$. We model $\mathbf{b}(\boldsymbol{\delta}, \mathbf{v}_{b/w}^b) = [F_x, F_z, \tau_x, \tau_y, \tau_z]^\top$ with the equations

$$F_x(\boldsymbol{\delta}, \mathbf{v}_{b/w}^b) = \sum_{i=1}^{3} \cos(\xi_{ri}) T_p(\delta_{ri}, \mathbf{v}_{b/w}^{ri}) + \Gamma(V_a)(\sin(\alpha)C_{L_{\delta_e}} - \cos(\alpha)C_{D_{\delta_e}})(\delta_{e1} + \delta_{e2}) \quad (7a)$$

$$F_z(\boldsymbol{\delta}, \mathbf{v}_{b/w}^b) = -\sum_{i=1}^{3} \sin(\xi_{ri}) T_p(\delta_{ri}, \mathbf{v}_{b/w}^{ri}) - \Gamma(V_a)(\cos(\alpha)C_{L_{\delta_e}} + \sin(\alpha)C_{D_{\delta_e}})(\delta_{e1} + \delta_{e2}) \quad (7b)$$

$$\tau_x(\boldsymbol{\delta}, \mathbf{v}_{b/w}^b) = -\sum_{i=1}^{3} \sin(\xi_{ri}) T_p(\delta_{ri}, \mathbf{v}_{b/w}^{ri}) q_{i,y} - \sum_{i=1}^{3} \cos(\xi_{ri}) Q_p(\delta_{ri}, \mathbf{v}_{b/w}^{ri}) + \Gamma(V_a) b C_{l_{\delta_a}}(-\delta_{e1} + \delta_{e2}) \quad (7c)$$

$$\tau_y(\boldsymbol{\delta}, \mathbf{v}_{b/w}^b) = \sum_{i=1}^{3} (\cos(\xi_{ri}) q_{i,z} + \sin(\xi_{ri}) q_{i,x}) T_p(\delta_{ri}, \mathbf{v}_{b/w}^{ri}) + \Gamma(V_a) c C_{m_{\delta_e}}(\delta_{e1} + \delta_{e2}) \quad (7d)$$

$$\tau_z(\boldsymbol{\delta}, \mathbf{v}_{b/w}^b) = -\sum_{i=1}^{3} \cos(\xi_{ri}) T_p(\delta_{ri}, \mathbf{v}_{b/w}^{ri}) q_{i,y} + \sum_{i=1}^{3} \sin(\xi_{ri}) Q_p(\delta_{ri}, \mathbf{v}_{b/w}^{ri}), \quad (7e)$$

where α is the angle of attack which can be found from the airspeed vector, $C_{L_{\delta_e}}$, $C_{D_{\delta_e}}$, and $C_{m_{\delta_e}}$ are the elevator aerodynamic coefficients of lift, drag, and pitch, $C_{l_{\delta_a}}$ is the aileron aerodynamic roll coefficient, $\Gamma(V_a) = \frac{1}{2}\rho V_a^2 S$, ρ is the air density, V_a is the airspeed magnitude, S is the wing surface area, b is the wingspan, and c is the wing's standard mean chord.

III. Control Allocation Scheme

We compare the nonlinear, low-energy-actuator-prioritizing control allocation we present in this work with the linear model used in [2]. A brief description of this linear representation and least-squares pseudoinverse method for computing control allocation will be given here to contrast the nonlinear method we have developed.

The psuedoinverse method uses the linear B matrix to approximate thrust and torque achieved by the vehicle's actuators. This method calculates the setpoint vector, $\boldsymbol{\delta}$, with the minimum norm needed to achieve the desired thrust and torque. In an unconstrained and linear problem, this would result in each of the actuators being set as low as possible in order to achieve the desired force and torque. This is shown by

$$B\boldsymbol{\delta} = \begin{bmatrix} \boldsymbol{F}_d^b \\ \boldsymbol{\tau}_d^b \end{bmatrix}, \quad (8)$$

where $\boldsymbol{F}_d^b$ is the desired force vector in the body frame and $\boldsymbol{\tau}_d^b$ is the desired torque vector in the body frame. The actuator setpoint vector, $\boldsymbol{\delta}$, is solved for using a minimum norm pseudoinverse solution to Equation 8.

The pseudoinverse method is limited by its inability to account for actuator saturation or for the nonlinearities in the thrust and torque produced by each rotor. This can result in the controller repeatedly allocating insufficient power to its actuators causing desired thrusts and torques to not be achieved, even when the thrust and torque combination may be achievable by the vehicle, causing poor tracking performance or loss of control.

To make the eVTOL controller robust against actuator saturation and the nonlinearities of rotor thrusts/torques at fixed-wing airspeeds, we developed a nonlinear control allocation scheme using an iterative optimization algorithm. Not only does this protect control allocation from saturation problems and inaccuracies caused by nonlinear actuators, this method also allows us to prioritize use of energy efficient actuators yielding better energy-use in these vehicles.

This control allocation method uses a nonlinear, iterative optimization algorithm to determine the actuator setpoints that will result in the thrust and torque being achieved with minimal use of high-energy rotors. This is described by

$$\begin{aligned} \min\ & \frac{1}{2}\left[\begin{bmatrix}\boldsymbol{F}_d^b\\ \boldsymbol{\tau}_d^b\end{bmatrix} - \mathbf{b}\left(\boldsymbol{\delta}, \mathbf{v}_{b/w}^b\right)\right]^\top K_\tau \left[\begin{bmatrix}\boldsymbol{F}_d^b\\ \boldsymbol{\tau}_d^b\end{bmatrix} - \mathbf{b}\left(\boldsymbol{\delta}, \mathbf{v}_{b/w}^b\right)\right] \\ & + [\boldsymbol{\delta}_{\text{ideal}} - \boldsymbol{\delta}]^\top K_\delta [\boldsymbol{\delta}_{\text{ideal}} - \boldsymbol{\delta}], \\ \text{subject to } & \boldsymbol{\delta}_{\min} \leq \boldsymbol{\delta} \leq \boldsymbol{\delta}_{\max}, \end{aligned} \tag{9}$$

where $K_\tau \in \mathbb{R}_{5\times5}$ specifies the priorities of different axes, $K_\delta \in \mathbb{R}_{7\times7}$ specifies priorities of actuator use, and $\boldsymbol{\delta}_{\text{ideal}}$ is the actuator setpoint configuration where no energy is used. The elements of the K_δ matrix are much smaller than the weighting matrix, K_τ. Thus, the primary optimization effort goes toward minimizing the difference between desired and achieved thrusts/torques, while the secondary objective minimizes certain actuators. In the simulation results described in this paper, we have used $K_\tau = I_{5\times5}$, and K_δ is a diagonal matrix with 1e-6$V_a^2[10, 10, 10, .3, .3, 0, 0]$ along the diagonal. This K_δ minimizes thrust produced by the rotors which then prioritizes using the vehicle's elevons to produce lift and torque. We include the V_a^2 term to reflect how the elevons gain effectiveness in producing force and torque as airspeed increases.

To minimize the cost function shown in Equation (9), we use a constrained, Broyden-Fletcher-Goldfarb-Shanno (BFGS) optimization algorithm [9]. The BFGS algorithm uses an initial guess as a start and then iterates until a suitable solution is found or a maximum number of iterations is reached. We have chosen to use a smaller maximum number of iterations because of the high update frequency of the control allocation module, and we use the previous solution as the next initial guess. Although iterative optimization algorithms can take relatively long, the small number of iterations combined with the high update rate allows this method to be an effective solution for finding optimal actuator setpoints. Our simulation results have shown that even when the number of iterations reaches the maximum limit, differences between achieved and desired wrenches are most often negligible. In rare cases when desired forces and torques are not achieved, the rate control integrators account for unachieved torques and the optimization is quickly able to converge in subsequent time-steps.

IV. Software Implementation and Simulation Results

A. Software Implementation and Simulation Environment

We have chosen a combination of ROS2 and the popular PX4 Autopilot Software [10] as platforms for implementing the controller described in [2] with the nonlinear control allocation method presented in this work. The control diagram is shown in Figure 2.

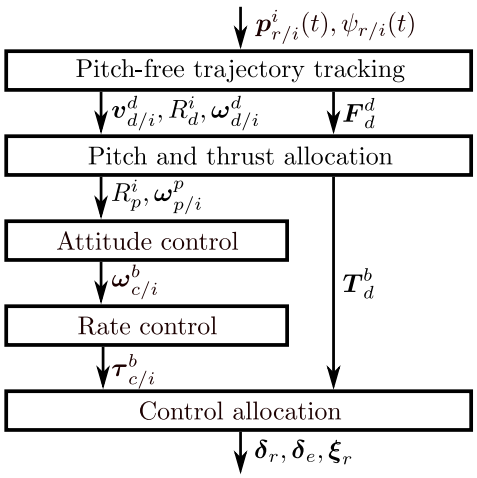

Fig. 2. Control diagram for eVTOL flight controller for all flight regimes (take-off, cruise, and landing). The controller tracks a trajectory of time-bound positions and headings. The control allocation piece receives a desired thrust from the pitch and thrust allocation and a desired torque from the rate control and outputs actuator setpoints.

The trajectory generation and trajectory tracking pieces of the controller are implemented as ROS2 nodes. These nodes communicate with PX4 software in companion-computer-mode through a microRTPS (Real Time Publish Subscribe) connection. The attitude control, rate control, and our custom control allocation piece are coded in C++ in adjusted PX4 Autopilot Software. We use an altered, constrained BFGS algorithm from the OptimLib C++ open-source library [11].

To simulate the control allocation method described in this paper, we use an enhanced version of AirSim, a powerful, visually realistic, open-source simulation environment built on the Unreal Engine graphics software, shown in Figure 3. AirSim previously only ran simulations for quadrotor and rover vehicles; however, we have added the capability to run eVTOL simulations using our custom tiltrotor graphical mesh and the aerodynamic model described in Section II. Note that the simulation dynamics use a tri-tiltrotor eVTOL model even though the aircraft graphic does not show the

rear rotor because the graphical mesh was originally designed for a twin-tiltrotor eVTOL vehicle. This visually realistic environment will be particularly helpful for future work that seek to integrate camera information into dynamic trajectory generation. This environment allows us to perform time-constrained, software-in-the-loop testing.

Fig. 3. Tiltrotor eVTOL vehicle flying in AirSim simulation environment using our ROS2 trajectory tracker and altered PX4 Autopilot Software.

B. Simulation Results

To demonstrate the tracking improvements made by the nonlinear, low-energy-actuator-prioritizing control allocation method, we simulate a trajectory involving vertical take-off, transition to and from high-airspeed (top speed of 27.9 m/s), fixed-wing flight, and vertical landing. We show the performance of the pseudoinverse method and the nonlinear, low-energy-actuator-prioritizing optimization method along the trajectory in Figure 4.

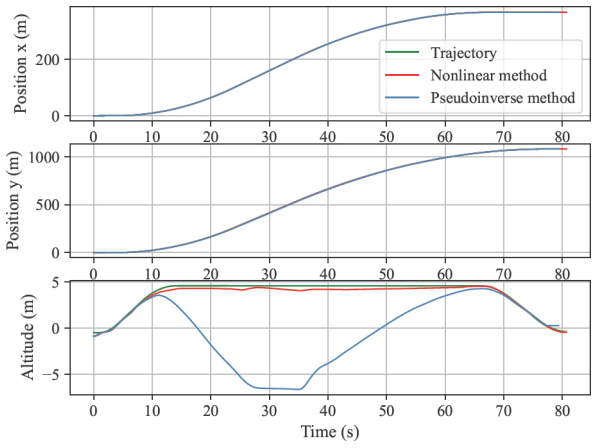

Fig. 4. Simulated positions of eVTOL aircraft using nonlinear optimization and pseudoinverse control allocation methods to track fast-flight trajectory.

The trajectory position error is shown rotated by the heading into the vehicle-1 frame of the trajectory in Figure 5. For this trajectory, the error vector has an average magnitude of 0.44 m for the nonlinear control allocation while the pseudoinverse method has an average error of 4.4 m. The error in the pseudoinverse method is primarily seen in the altitude and along the vehicle-1 x-axis. The linear rotor model's inaccuracies keep the vehicle using the pseudoinverse control allocation method from keeping up with the trajectory, and the pseudoinverse method's inability to cope with saturation keeps the vehicle from achieving the desired pitch as is seen in the attitude error plots in Figure 6.

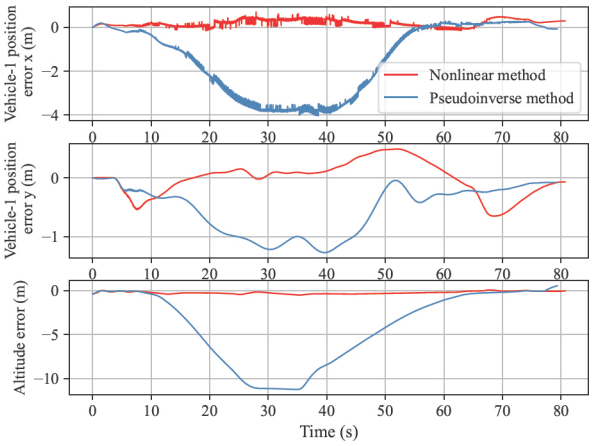

Fig. 5. Position error rotated into the vehicle-1 frame of the trajectory. The simulation of the pseudoinverse control allocation method experiences much greater error in the vehicle-1 x-axis and altitude tracking than the nonlinear optimization method.

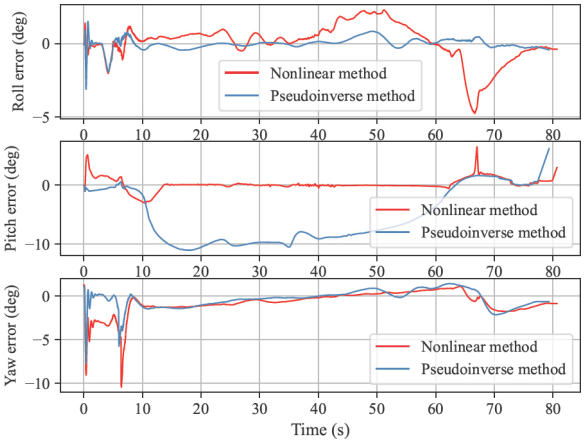

Fig. 6. Attitude error of nonlinear optimization and pseudoinverse control allocation methods. The pseudoinverse method struggles to allocate the torque needed to maintain pitch.

We also show the actuator setpoints across the trajectory in Figure 7. We include plots of the actuator setpoints for the non-

linear method without efficient actuator prioritization to show that the nonlinear, low-energy-actuator-prioritizing method is able to use similar energy to that of the pseudoinverse method while maintaining much better tracking results. The nonlinear method with actuator prioritization uses on average 7% less throttle than the nonlinear method without prioritization. In the pseudoinverse method plots, the low-bound saturation of the rear rotor (δ_{r3}) can be seen. This saturation causes the vehicle to lose altitude and be unable to maintain pitch. Additionally, the prioritization of energy-efficient actuators allows greater use of the control surfaces, as can be seen from the elevons receiving setpoints of greater magnitude in our nonlinear optimization control allocation method.

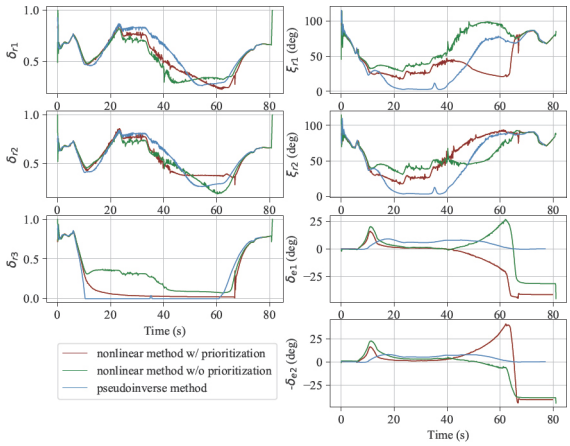

Fig. 7. Actuator setpoints along the simulated fast-flight trajectory used in this section. The results from the nonlinear optimization method are shown when low-energy actuators are prioritized and when no prioritization is used. While the front two rotors experience similar use between all three methods shown, the throttle of the rear rotor is able to be set much lower in the pseudoinverse and nonlinear method with low-energy-actuator-prioritization than in the nonlinear method without prioritization. On average, the nonlinear actuator prioritizing method uses 36% less rear rotor throttle and 7% less total rotor throttle than the nonlinear method without prioritization.

V. Conclusion

We have developed a nonlinear, low-energy-actuator-prioritizing control allocation method for eVTOL aircraft that uses a bounded, iterative nonlinear optimization algorithm to find optimal actuator control points. This method accounts for actuator limits to avoid saturation and uses nonlinear rotor and control surface representations to model actuators with greater accuracy. Our simulation results show a significant improvement from pseudoinverse control allocation techniques. In addition to giving greater control precision, this method allows for more flexibility with prioritizing certain axes and actuators. The high update rate and use of the previous setpoints as the algorithm's next initial guess make this nonlinear scheme feasible in hardware.

Future works include dynamically prioritizing rotors when angle of attack gets too high to maintain better control at close-to-stall speeds, testing the controller in hardware, and making the control allocation more robust to uncertain aerodynamic parameters.

References

[1] T. A. Johansen and T. I. Fossen, "Control allocation—a survey," *Automatica*, vol. 49, no. 5, pp. 1087–1103, May 2013.

[2] J. Willis and R. W. Beard, "A nonlinear trajectory tracking control for winged eVTOL UAVs," in *Proceedings of the American Control Conference*, June 2021, pp. 1683–1688.

[3] T. Lombaerts, J. Kaneshige, S. Schuet, G. Hardy, B. L. Aponso, and K. H. Shish, "Nonlinear dynamic inversion based attitude control for a hovering quad tiltrotor eVTOL vehicle," in *AIAA Scitech 2019 Forum*. American Institute of Aeronautics and Astronautics, jan 2019.

[4] M. J. Acheson, I. M. Gregory, and J. Cook, "Examination of unified control incorporating generalized control allocation," in *AIAA Scitech 2021 Forum*. American Institute of Aeronautics and Astronautics, jan 2021.

[5] X. Shi, K. Kim, S. Rahili, and S.-J. Chung, "Nonlinear control of autonomous flying cars with wings and distributed electric propulsion," *IEEE Conference on Decision and Control (CDC)*, pp. 5326–5333, 2018.

[6] S. Shah, D. Dey, C. Lovett, and A. Kapoor, "Airsim: High-fidelity visual and physical simulation for autonomous vehicles," in *Field and Service Robotics*, M. Hutter and R. Siegwart, Eds. Cham: Springer International Publishing, 2018, pp. 621–635.

[7] R. Anderson, J. Willis, J. Johnson, A. Ning, and R. W. Beard, "A comparison of aerodynamics models for optimizing the takeoff and transition of a bi-wing tailsitter," in *AIAA Scitech 2021 Forum*, 2021, p. 1008.

[8] J. Willis, J. Johnson, and R. W. Beard, "State-dependent LQR control for a tilt-rotor UAV," in *2020 American Control Conference (ACC)*, 2020, pp. 4175–4181.

[9] J. Nocedal and S. J. Wright, *Numerical Optimization*, 2nd ed. New York, NY, USA: Springer, 2006.

[10] L. Meier, D. Honegger, and M. Pollefeys, "PX4: A node-based multithreaded open source robotics framework for deeply embedded platforms," *2015 IEEE International Conference on Robotics and Automation (ICRA)*, pp. 6235–6240, 2015.

[11] K. O'Hara, "Optimlib," https://www.kthohr.com/optimlib.html, 2017.